Thermodynamic properties of the actinide metals Th and U: A first-principles study

Li Li and Yi Wang
Institute of Applied Physics and Computational Mathematics P.O. Box 8009, Beijing, 100088 People's Republic of China
(Received 14 April 2000; revised manuscript received 9 January 2001; published 4 June 2001)

Utilizing a combination of first-principles electronic structure calculation and the recently developed mean-field potential approach, we have calculated the static 300 K equation-of-state, the dynamic Hugoniot equation-of-state, and the major thermodynamic properties along the principal Hugoniot for actinide metals Th and U. We demonstrate that the modern first-principles technique can describe most of the thermodynamic quantities within the experimental error bars even for the two heaviest $5f$ metals at pressures up to 1000 GPa and temperatures up to $\sim$74 000 K for Th and $\sim$42 000 K for U.

DOI: 10.1103/PhysRevB.63.245108 PACS number(s): 71.15.Nc, 05.10.−a, 05.70.Ce, 71.15.Ap

I. INTRODUCTION

Over the past decades, density-functional theory[1,2] has successfully provided a framework within which ground-state properties of many physical systems can be calculated.[3–10] However, *ab initio* thermodynamic studies, especially for the *f*-electron systems, still remain a great challenge to us. This paper is concerned with the calculation of the thermodynamic properties of the actinide metals Th and U, where Th is unique in being a transition metal with s-d hybridization and on the threshold of being a regular $5f$ band light actinide element and U is unique in being in the central part of the strong *f*-bond metals and the heaviest naturally occurring element. There are two main motivating factors behind this paper.

First, the current testing ground for electronic structure theory of the elements is the actinide metal, the last period of the Periodic Table. Two important topics in the condensed state science of the actinide elements are the electron configuration and the nature of the bonding in their metals.[8–11] The thermodynamic property studies of actinide metals would be very valuable for elucidating their electronic behavior and atom-atom interactions.

Second and most important, the equation-of-state (EOS), namely, the relationship of pressure-volume-temperature (P,V,T), is one of the most basic physical properties of a substance. Historically a lot of attention[12–20] has been focused on this thermodynamic behavior and recent progress in x-ray diffraction with synchrotron radiation and diamond-anvil cells has extended the range for accurate lattice parameter determinations into the multimegabar region exceeding 300 GPa.[17] To interpret the dynamic as well as static high-pressure experiments and to study the specific behaviors of a substance when undergoing severe constraints such as high-pressure and high-temperature environments, the development of an accurate *ab initio* EOS model, where only the atomic number is taken as the ''adjustable parameter,'' is currently of immense importance. Although workers have been engaging in the first-principles calculations for actinides over the past two decades, few attempts are made to calculate the dynamic shock-wave compressed properties for actinides in the *ab initio* scenario while the shock-wave experiment might be one of the most efficient ways to explore the thermodynamic properties of a substance at ultrahigh pressures and temperatures. The present paper is unique in this regard.

The study of the temperature dependence of the properties of materials requires a proper account of nuclear motions and thermal excitation of electrons. In a series of papers,[21–23] we have developed a classical mean-field potential (MFP) approach to calculate the various kinds of thermodynamic quantities of a metal. With the well-known Dugdale and MacDonald[24] expression for the Grüneisen constant being explicitly deduced, the MFP approach was first tested on the metal Ce, indicating that the well-known γ-α isostructural transition, the experimental Hugoniot state, and the 300 K static equation-of-state were well reproduced.[21] The MFP approach was then checked on the five reference metals Al, Cu, Ta, Mo, and W, indicating that both the calculated Hugoniot states and 293 K isotherms fell well within the experimental uncertainties.[22] Consecutively, the MFP approach was expanded to more general cases,[23] where as the second-order approximation of the MFP, the three commonly used expressions for the Grüneisen parameter, i.e., that due to Slater,[25] that due to Dugdale and MacDonald, and that for the free-volume theory,[26] were all explicitly deduced on a common physical basis. The calculation[23] on metallic Al might be the best demonstration, where the MFP approach correctly described most of the thermodynamic properties, such as static compression, shock-wave compression, thermal expansion, bulk modulus, and the anharmonic effect.[27,28] These promising results have encouraged us to study the $5f$ series.

The rest of this paper is organized as follows. In Sec. II we present a brief description of the MFP approach. Section III describes the calculational parameters. In Sec. IV we discuss our results for Th. In Sec. V we discuss our results for U. Finally, Sec. VI contains our summary.

II. THERMODYNAMIC MODEL

For a substance, if we have the Helmholtz free energy as an explicit function of volume and temperature, we can calculate all other thermodynamic parameters. Let us consider a system with a given averaged atomic volume V and temperature T. The Helmholtz free-energy $F(V,T)$ per ion can be written as[29]

$$F(V,T)=E_c(V)+F_{ion}(V,T)+F_{el}(V,T), \qquad (1)$$

where E_c represents the 0 K total energy, F_{ion} the vibrational free energy of the lattice ion, and F_{el} the free energy due to the thermal excitation of electrons.

With the previous work,[21,26] F_{ion} is

$$F_{ion}(V,T) = -k_B T\left[\frac{3}{2}\ln\frac{mk_BT}{2\pi\hbar^2} + \ln v_f(V,T)\right], \qquad (2)$$

with

$$v_f(V,T) = 4\pi\int \exp\left[-\frac{g(r,V)}{k_BT}\right]r^2dr. \qquad (3)$$

The central issue of the mean-field theory is how to calculate the MFP $g(r,V)$. In this regard, the free-volume theory[26] chose to calculate the MFP $g(r,V)$ by the average of the empirically derived pairwise potentials, while the tight-binding total-energy classical cell model[30] chose to calculate the MFP $g(r,V)$ by the tight-binding total-energy method for which all the parameters were determined by the first-principles full-potential linearized augmented plane wave (LAPW) calculation.

Inspired by the three commonly used expressions for the Grüneisen parameter,[24–26] we have simply constructed the MFP in terms of the *ab initio* 0 K total energy E_c as follows:[21,23]

$$g(r,V) = \frac{1}{2}[E_c(R+r)+E_c(R-r)-2E_c(R)] + \frac{\lambda}{2}\frac{r}{R}[E_c(R+r)-E_c(R-r)], \qquad (4)$$

where r is the distance that the lattice ion deviates from its equilibrium position and R is the lattice constant with respect to V.

The physical basis of Eq. (4) can be demonstrated by the fact that the three commonly used expressions for the Grüneisen parameter, i.e., that due to Slater ($\lambda=-1$), that due to Dugdale and MacDonald ($\lambda=0$), and that for the free-volume theory ($\lambda=1$), can all be explicitly deduced if we take the second-order approximation to Eq. (4).

III. CALCULATIONAL PARAMETERS

To calculate the 0-K total energy $E_c(V)$ in Eq. (1), the LAPW method[3] within the generalized gradient approximation[4] is employed. The calculation of F_{el} follows the previous work.[21–23] To examine the effects of the choices of the MFP in Eq. (4) (or equivalently λ) on the calculated results, all the three MFP, namely, $\lambda=-1$, $\lambda=0$, and $\lambda=1$, have been tested. We note that we do not make any attempts to analytically fit the LAPW calculated points since the fitting might alter the original LAPW results. In all the thermodynamic calculations, the LAPW calculated numerical points are directly taken as the input, then more dense points in the lattice constant step of 0.005 a.u. are derived by cubic spline interpolation for the convenience of one-dimensional numerical enumeration. Out of the lattice constant region of the LAPW calculations, the Lennard-Jones function extrapolation towards the zero and the Morse function extrapolation towards infinite are invoked to get the 0 K energy curve.

In Th, the ambient structure is fcc. Under compressions, the recent experimental work by Vohra and co-workers[17] demonstrated that it continuously transformed from fcc to bct form from 63.7 GPa. To respond to these, we have studied the fcc structure, as well as three bct structures with the c/a ratios of 1.477, 1.563, and 1.655.

At ambient conditions, U takes, with two atoms in the unit cell, the face-centred orthorhombic structure (α-U)[18,31,32] which keeps stable at least up to 100 GPa at compressions. At higher pressures, the previous calculation[9] assumes that U would undergo the transitions, first to the bct structure and then to the bcc structure, although there are no experimental proofs. In this paper, all these structures are considered. More specifically, for α-U, we use the internal crystallographic coordinate ratios of Ref. 31, and for bct-U we use the c/a ratio of 0.82 suggested by Söderlind *et al.*[9] (our preliminary calculations indeed show that this is the optimized value).

With regard to the parameters in the 0 K calculation, the major ones are the muffin-tin radii R_{mt} and the energy parameters. In general, it is a common practice to use a constant R_{mt} in the LAPW method,[10] whereas a varied R_{mt}, which makes the ratio of the volume of the muffin-tin sphere to the volume of the atom a constant, in the LMTO (linear-muffin-tin-orbital) method.[9] Accordingly, we use the constant value of 2.0 a.u. for R_{mt}. For the energy parameters, there are some ambiguities. We choose to use the values in their respective band centers. This means that two steps of calculations are performed, where the first step is run to self-consistency to find the best energy parameters, which are served as the input of the second step (also being run to self-consistency).

The other parameters needed in the 0 K calculation are as usual. The plane-wave cutoff K_{cut} is determined by $R_{mt}\times K_{cut}=9.0$. On reciprocal-space integrations in the full Brillouin zone, we use 8000 k points for fcc and bcc structures and 1000 k points for bct and α-U structures. The calculations are performed for atomic volumes ranging from 50% expansion down to about threefold compression. The valent basis sets include the $7s$, $7p$, $6d$, and $5f$ partial waves, and local orbitals[3] are added to enhance the variational freedom and allow the semicore $5d$, $6s$, and $6p$ orbitals to be treated along with the valence electrons, with the additional energy parameter used to simultaneously treat the residual s and p character of the valence electrons. The remaining electrons are considered as belonging to the core, but their wave functions are relaxed, i.e., recalculated in each iteration.

IV. THORIUM

A. Thermodynamic properties under ambient conditions and the impact of calculational parameters on the calculated results

We also discuss the calculated ambient properties of U here for the convenience of discussions. Collected in Table I

TABLE I. The calculated and experimental atomic volumes V_0 (in Å^3), bulk moduli B (in GPa), and volume thermal-expansion coefficients β (in 10^{-6}/K) of ambient conditions for Th and U.

	Th			U		
λ	V_0	B	β	V_0	B	β
−1	32.50	59.2	33.9	21.49	116.7	31.2
0	32.43	59.8	25.8	21.46	117.2	26.3
1	32.37	60.2	17.9	21.42	117.5	21.4
Expt.	32.87[a]	54.0-59.0[b]	33.6[c]	20.75[a]	135.5,[d] 125,[e] 115[f]	37.8[c]

[a]From Ref. 33.
[b]From Ref. 17.
[c]From Ref. 34.
[d]From Ref. 18.
[e]From Ref. 19.
[f]From Ref. 35.

are our calculated atomic volumes (V_0), bulk moduli (B), and volume thermal-expansion coefficients (β) under ambient conditions together with the measured data.[17–19,33–35]

For Th, our calculation reproduces the computed equilibrium atomic volume of Jones *et al.*[10] But for U, our calculated V_0 is ~3% greater than that by Jones *et al.* The disagreement can be understood in sense of the choices of the energy parameters, considering that the $5f$ orbitals form very narrow bands close to the Fermi level. For Th, the way of choosing the energy parameters does not have visible effects on the calculated results since Th can be viewed as an *s-d* metal. However for U, the situation becomes severe since U is a strong *f*-bond metal. Jones *et al.* chose to use the fixed values that were set near the centers of their respective bands by monitoring the eigenvalues of the calculation whose volume lay closest to equilibrium. However, since in our case we are engaged in the EOS calculations at pressures up to 1000 GPa, the usages of the fixed energy parameters for all the considered volumes are evidently impractical. We note that in our calculation, for a given volume we always use the energy parameters that are in their respective band centers.

As regards the effects of the choices of the MFP (or equivalently λ) on the calculated results, from Table I we can find that they are strong on β. Choosing λ reminds us of the choices[7,36,37] among the three expressions[24–26] of the Grüneisen parameter. Söderlind *et al.*[36] had found that the Slater expression was more suitable for the light actinide than the other two expressions.

We may mention here that the above-mentioned discrepancies do not persist as the serious problems to the calculations in the following sections due to the fact that (i) we can use the reduced atomic volume V/V_0, (ii) at low temperature and pressure the thermal parts in Eq. (1) are considerably small compared to the cold part, and (iii) at high temperature and pressure the effects of the different choices of the MFP on the calculated results become small (see the sections for calculations of the Hugoniot states).

B. The phase stability under compressions

The calculated 300 K Gibbs free energies of bct structures with the c/a ratios of 1.477, 1.563, and 1.655 are illustrated in Fig. 1 taking that of the fcc structure as the zero. Notice the experimental results[17] that the fcc-bct transition is continuous and the bct structure with $c/a=1.655$ is the most preferable for ultrahigh compressions are reproduced rather well.

At the transition pressure of ~100 GPa, our calculated volume collapse by $\Delta V/V_0$ is 0.8%. Although this collapse is too small to be observed by the experimental accuracy, it indeed makes the agreements between the calculations and the experiments better (see Fig. 2).

C. 300 K static equation-of-state

The calculation of the 300 K static EOS can serve as a good check of the accuracy of the 0 K calculation since the 300 K static EOS is dominated by the $T=0$ energetics and the thermal contribution is very small. Therefore for the 300 K static EOS, we will only discuss the calculated results using $\lambda=0$ in Eq. (4). For Th, Vohra, and co-workers[17] had given measured data up to 300 GPa, McQueen and Marsh[15] had given shock-reduced 300 K isotherm up to 150 GPa, and Kennedy and Keeler[14] had given a shock-reduced 298 K isotherm up to 100 GPa in the *AIP Handbook*. The calculated results for the fcc structure and the bct structure with $c/a=1.655$ are plotted in Fig. 2 together with these experimentally based data.

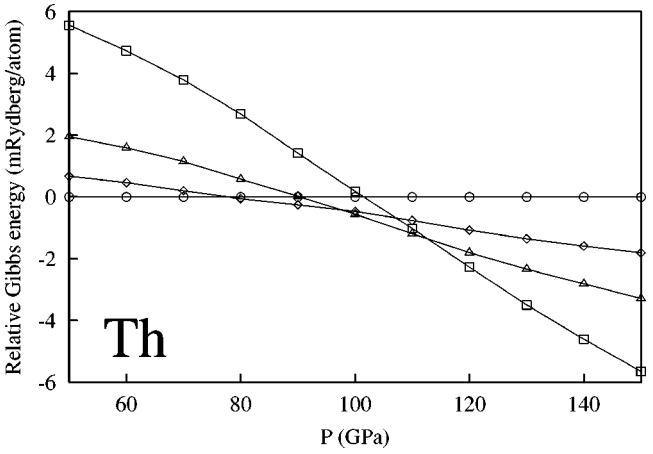

FIG. 1. The calculated 300 K relative Gibbs free-energy of Th under compressions. The circles represent those using the fcc structure, which has been taken as the reference zero point. The diamonds, triangles, and squares represent those using the bct structures with $c/a=1.477$, 1.563, and 1.655, respectively.

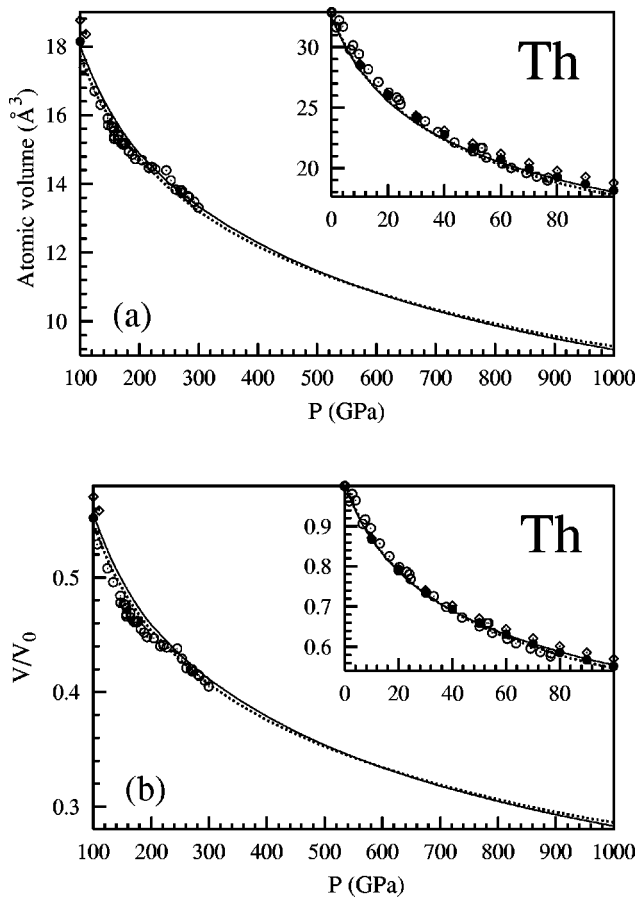

FIG. 2. The 300 K static EOS for Th. (a) V-P plot. (b) V/V_0-P plot. The solid line represents the calculated result using the fcc crystal and the dotted line represents the calculated result using the bct crystal ($c/a=1.655$). The solid circles are from Kennedy and Keeler (Ref. 14), the open circles are from Vohra and Holzapfel (Ref. 17), and the diamonds are the shock-reduced data by McQueen and Marsh (Ref. 15).

Generally speaking, at present it is somewhat difficult by first-principles method to derive the calculated atomic volumes within the experimental error bars. For instance, an accuracy of 1% in the lattice constant by first-principles calculation is considered to be rather excellent especially for the actinide metals, however, this accuracy means an error of 3% in the atomic volume or density. Therefore, we employ two types of plots: they are the curve of the atomic volume V versus the pressure P [Fig. 2(a)] and the curve of the reduced atomic volume V/V_0 versus the pressure P [Fig. 2(b)]. The use of the V/V_0-P plot for the comparison of the calculation and the experiment is especially suitable according to the present calculation and our previous work.[22] Note that in Fig. 2(b), our calculated results exactly go through the shock-reduced 298 K isotherm by Kennedy and Keeler, which had been claimed to have an accuracy as high as 5% in pressure. And, we may note, that the traditional ways by McQueen and Marsh[15] for the reductions of the shock-wave data of Th, might not be suitable for high compressions when the thermal electronic contributions were neglected.

D. Hugoniot state

Hugoniot states, which are derived by the conventional shock-wave technique,[12] are characterized by using measurements of shock velocity (D) and particle velocity (u) with $V_H/V_0=(D-u)/D$ and $P_H=\rho_0 Du$, where P_H is the pressure and ρ_0 is the initial density. Through the Rankine-Hugoniot relations, these data define a compression curve [volume (V_H) versus pressure (P_H)] as a function of known Hugoniot energy (E_H):

$$\tfrac{1}{2}P_H(V_0-V_H)=E_H-E_0, \tag{5}$$

where V_0 and E_0 refer to the atomic volume and energy at ambient conditions, respectively.

Unlike the static EOS, the temperature along the Hugoniot can undergo a range from room temperature to several tens of thousands of degrees, thus the calculations of the Hugoniot state could serve as a good check of a theoretical method for the thermodynamic calculation. Using the calculated V_0 and E_0 of the fcc structure, the Hugoniot EOS's for Th have been calculated at pressures up to 1000 GPa employing $\lambda=-1$, 0, and 1 for the fcc structure and $\lambda=0$ for the bct structure of $c/a=1.655$.

The calculated Hugoniot EOS's, together with the measured data from the Los Alamos compilation,[12] are compared in Fig. 3 for Th. We note that the differences among results using $\lambda=-1$, 0, and 1 are very small. Also shown in Fig. 3 are the Hugoniot data used in the reductions of shock-wave data by McQueen and Marsh.[15] By pressure against the atomic volume, the calculated results are only slightly lower than the experimental data. However, when we plot the EOS by pressure against the relative volume (V_H/V_0), our calculated curve of P_H versus V_H/V_0 for the fcc structure exactly goes through the data used by McQueen and Marsh [see Fig. 3(b)].

For high compression, it is unfortunate that no experimental data are found to further prove our calculation for Th. However, by the excellent agreements between the calculations and the experiments in our previous calculations,[21–23] in particular in the case of U in the following sections, we assume that our calculated curves of P_H versus V_H/V_0 can be adopted in the realistic application if the higher-pressure data are needed.

E. Grüneisen gamma along the principal Hugoniot

Since we have explicitly calculated the Helmholtz free-energy $F(V,T)$ as functions of V and T, all other thermodynamic parameters can be calculated. In particular, one can evaluate the thermodynamic Grüneisen gamma by

$$\gamma_{th}(T,V)=\frac{VB_T(V,T)\beta_P(V,T)}{C_V(V,T)}, \tag{6}$$

where B_T is the isothermal bulk modulus, β_P the thermal volume expansion coefficient, and C_V is the constant volume heat capacity, which should include both the lattice and the thermal electron contributions.

For releasing the concerns that might be raised by colleagues about the effects of the choices of the MFP in Eq. (4)

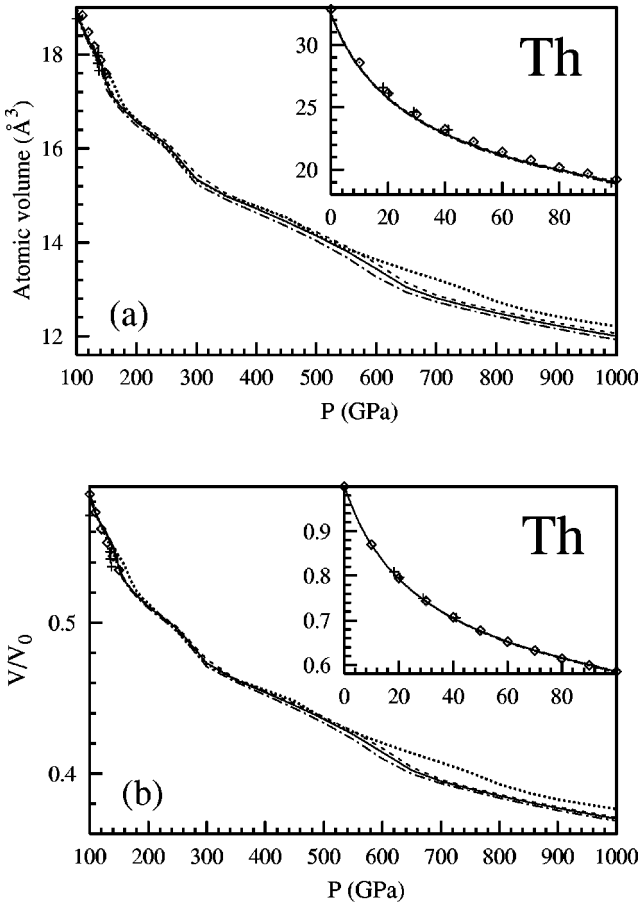

FIG. 3. Hugoniot EOS for Th. (a) V-P plot. (b) V/V_0-P plot. The dashed, solid, and the dot-dashed lines represent the calculated results for the fcc structure using $\lambda=-1$, 0, and 1, respectively. The dotted line represents the calculated result for the bct structure ($c/a=1.655$) using $\lambda=0$. The pluses are from the Los Alamos compilation (Ref. 12) and the diamonds the used data by McQueen and Marsh (Ref. 15). The inset illustrates the low compression region.

on the calculated results, the calculated γ_{th}'s with $\lambda=-1$, 0, and 1 for fcc Th are depicted in Fig. 4. One can immediately find that the differences among the calculated γ_{th}'s, using the three MFP's, are decreasing rapidly as the pressure is increasing, and only when the pressure reaches 100 GPa have these differences been smaller than 10% with respect to the value of γ_{th}. For pressure smaller than 100 GPa, the thermal pressure is very small compared with the cold pressure. As pointed out by Mitchell *et al.*,[37] metals shocked from ambient conditions remain in the solid state up to pressures of typically 100-200 GPa in which the EOS is dominated by the $T=0$ energetics. Altogether, these demonstrate that the calculated Hugoniot EOS would be rather insensitive to the choices of the MFP (see also the calculated results on the Hugoniot EOS and the temperature along the principal Hugoniot).

Workers may note that some structures appear along the calculated curves in Fig. 4. We can understand them if we note that

(i) The accurate calculation the Grüneisen gamma desires both extremely accurate energy-volume curve and extremely accurate electronic density-of-states (DOS) since it involves some products of the second-order derivatives of the 0 K data. We note again that in our thermodynamic calculations the LAPW calculated points are directly taken as the input, i.e., we do not make any attempts to analytically refit the LAPW calculated points. In this regard, the structures in Fig. 4 are, to the first grade, due to the computational artifacts.

(ii) At some pressure induced phase-transition points, although the same crystal structure is used, more or less a minor kink will appear in the 0 K energy-volume curve accompanying the large change of the electronic DOS near the Fermi level. A minor kink in the 0 K data would result in a large kink in the V-P data (see Fig. 3) and further an evident structure in the plot of the Grüneisen gamma. In this regard, the structures in Fig. 4 are, to the second grade, the reflection of some phase transitions.

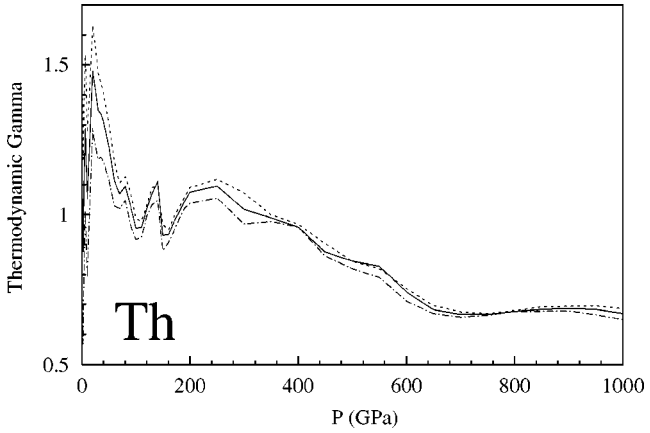

FIG. 4. The calculated thermodynamic Grüneisen gamma along the principal Hugoniot for Th. The dashed, solid, and the dot-dashed lines represent the calculated results for the fcc structure using $\lambda=-1$, 0, and 1, respectively.

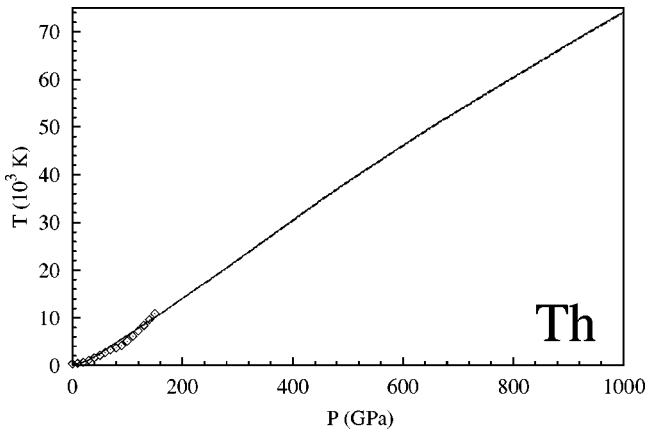

FIG. 5. The calculated temperature along the principal Hugoniot for Th. The dashed, solid, and the dot-dashed lines represent the calculated results for the fcc structure using $\lambda=-1$, 0, and 1, respectively. The diamonds are the shock-reduced data by McQueen and March (Ref. 15).

TABLE II. The calculated 300 K EOS, Hugoniot EOS, and Hugoniot temperature for Th.

	fcc			bct [a]		
	300 K	Hugoniot		300 K	Hugoniot	
P (GPa)	V/V_0	V/V_0	T (K)	V/V_0	V/V_0	T (K)
0.0	1.0000	1.0000	300	1.0049		
20.0	0.7861	0.7927	688	0.7885		
40.0	0.6899	0.7050	1787	0.6892		
60.0	0.6302	0.6516	3231	0.6241		
80.0	0.5877	0.6160	4776	0.5795		
100.0	0.5551	0.5846	6269	0.5471	0.5848	6207
120.0	0.5290	0.5645	7840	0.5205	0.5634	7805
140.0	0.5066	0.5504	9419	0.4995	0.5494	9421
160.0	0.4884	0.5278	10 894	0.4820	0.5377	11 011
180.0	0.4723	0.5182	12 476	0.4669	0.5209	12 556
200.0	0.4588	0.5106	14 071	0.4537	0.5126	14 137
250.0	0.4322	0.4960	18 064	0.4278	0.4937	18 148
300.0	0.4113	0.4732	22 158	0.4069	0.4727	22 180
350.0	0.3939	0.4620	26 324	0.3898	0.4621	26 318
400.0	0.3787	0.4538	30 487	0.3754	0.4554	30 448
450.0	0.3653	0.4452	34 581	0.3632	0.4481	34 519
500.0	0.3535	0.4361	38 539	0.3524	0.4363	38 499
600.0	0.3339	0.4142	46 171	0.3341	0.4203	46 053
700.0	0.3180	0.3950	53 466	0.3190	0.4074	53 266
800.0	0.3046	0.3853	60 490	0.3061	0.3929	60 296
900.0	0.2930	0.3771	67 382	0.2951	0.3830	67 159
1000.0	0.2830	0.3701	74 163	0.2860	0.3765	73 871

[a] $c/a=1.655$. V_0 is referred to that of fcc.

F. Temperature along the principal Hugoniot

In the traditional reduction of the Hugoniot data,[15,16] the temperature estimate remains less secure since it requires the accurate knowledge of specific heat and the Grüneisen parameter values that are not well known. In the MFP frame, all these quantities can be calculated straightforwardly. Figure 5 exemplifies the comparisons between the calculated Hugoniot temperatures and the shock-reduced results of Ref. 15 for fcc Th. We note again that the differences among results using $\lambda=-1$, 0, and 1 are negligible.

The calculated 300 K EOS, Hugoniot EOS, and temperature along the principal Hugoniot for fcc Th and bct Th ($c/a=1.655$) with $\lambda=0$, are listed in Table II for reference.

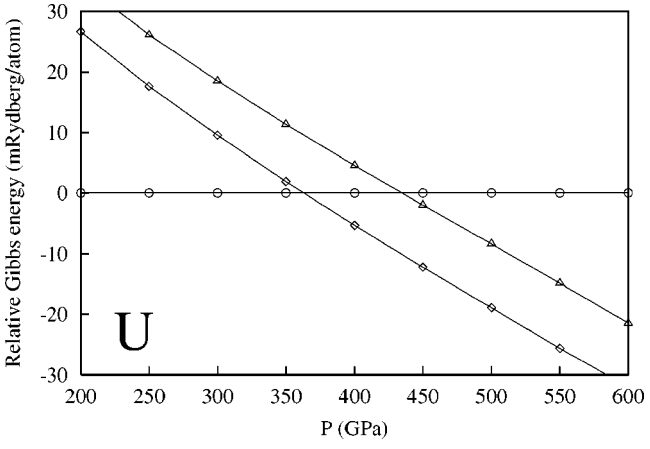

FIG. 6. The calculated 300 K relative Gibbs free-energy of U under compressions. The circles represent those using the α-U structure, which has been taken as the reference zero point. The diamonds represent those using the bct structure with $c/a=0.82$ and the triangles represent those using the bcc structure.

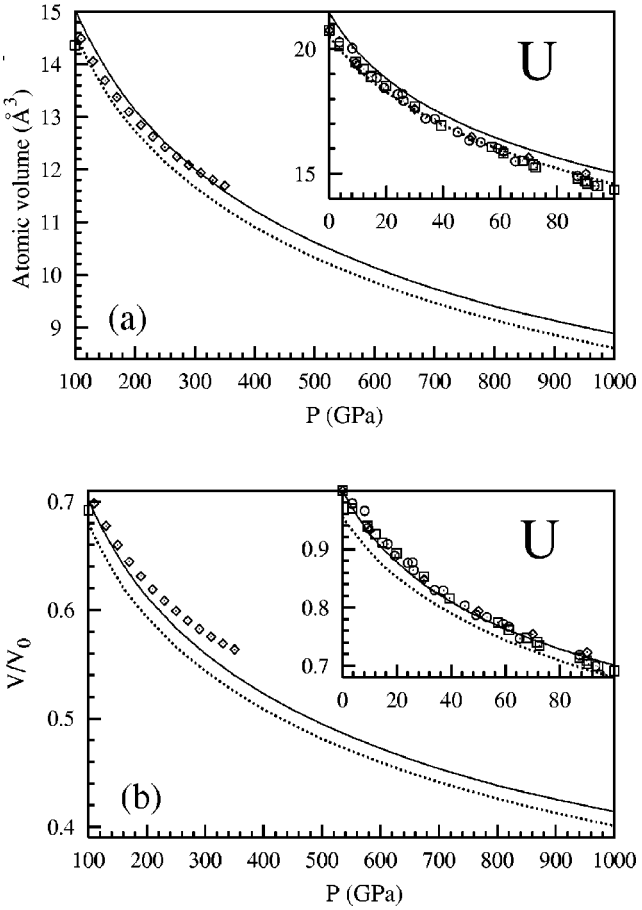

FIG. 7. The 300 K static EOS for U. (a) V-P plot. (b) V/V_0-P plot. The solid line represents the calculated result using the α-U crystal and the dotted line represents the calculated result using the bct crystal ($c/a=0.82$). The circles are from Yoo *et al.* (Ref. 18), the squares are from Akella *et al.* (Ref. 20), and the diamonds are the shock-reduced data (U-Mo alloy of 97% to 3% in weight) by McQueen *et al.* (Ref. 16).

V. URANIUM

A. The phase stability under compressions

The phase stabilities of uranium under compressions is somewhat a controversial issue. For light actinide metals Th, Pa, Np, and Pu, it had been confirmed that they underwent at least one structure transformation at pressure below 100 GPa. As U was positioned at the central part of the light actinide series, it was naturally considered that U would also show the similar behaviors.[19,38] However, the exceptional

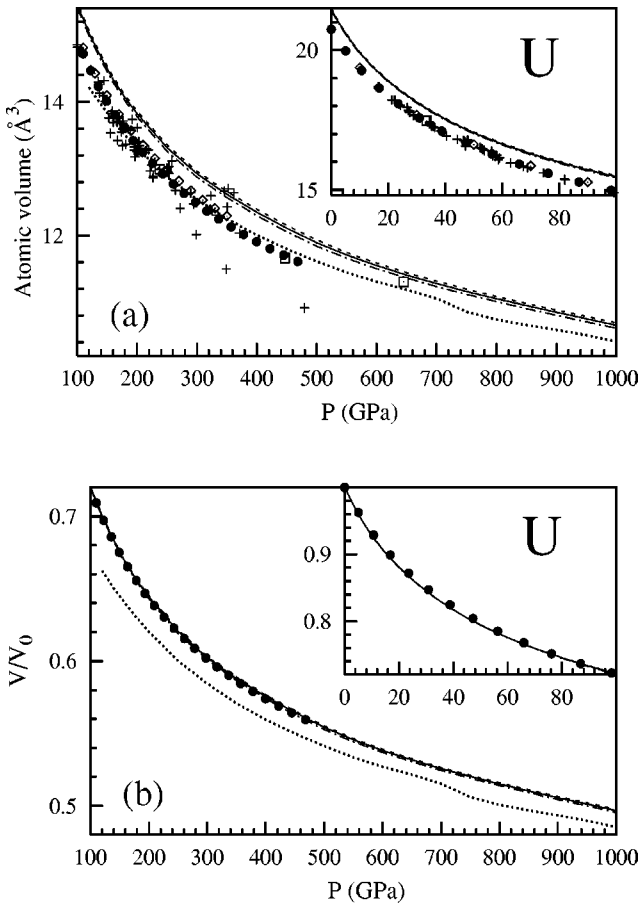

FIG. 8. Hugoniot EOS for U. (a) V-P plot. (b) V/V_0-P plot. The dashed, solid, and the dot-dashed lines represent the calculated results for the α-U structure using $\lambda=-1$, 0, and 1, respectively. The dotted line represents the calculated result for the bct structure ($c/a=0.82$) using $\lambda=0$. The pluses are from the Los Alamos compilation (Ref. 12), the squares from the LLNL Report (Ref. 13), the diamonds the used data (U-Mo alloy of 97% to 3% in weight) by McQueen *et al.* (Ref. 16), and the solid circles are derived from the $D-u$ fitting to the experimental data of $D=2.51+1.51u$ from Ref. 12.

case always occurs. The refined experiment and calculation recently by Akella *et al.*[32] show that the α-U is exceptionally stable at least up to 100 GPa.

The calculated 300 K Gibbs free energies of the bct ($c/a=0.82$) and the bcc structures are illustrated in Fig. 6 taking that of the α-U structure as the zero. We note that in our calculation we have not optimized the structure parameters of c/a, b/a, or y for α-U. Even so, our calculation shows that the α-U is the stablest up to the pressure of 363 GPa. For more higher pressures up to 1000 GPa, our calculation show that the bct ($c/a=0.82$) structure is preferable over both the α-U and the bcc structures.

B. 300 K static equation-of-state

Yoo *et al.*[18] had given measured data for U to 93 GPa, and Akella *et al.*[20] had given measured data for U to 100 GPa. The calculated results for the α-U structure and the bct

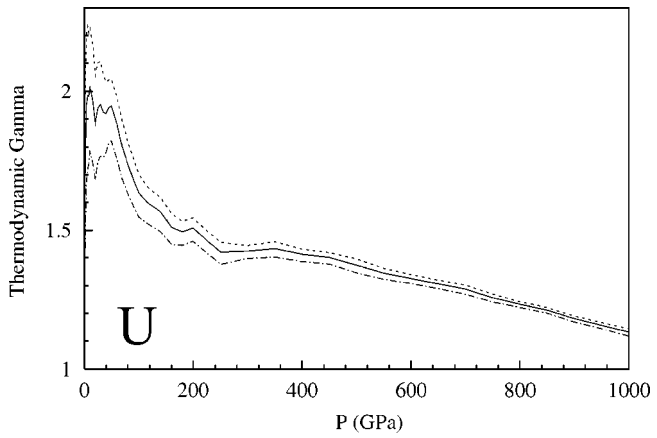

FIG. 9. The calculated thermodynamic Grüneisen gamma along the principal Hugoniot for U. The dashed, solid, and the dot-dashed lines represent the calculated results for the α-U structure using $\lambda=-1$, 0, and 1, respectively.

structure with $c/a=0.82$ are compared with these experimental data in Fig. 7, where the shock-reduced 300 K data for U-Mo alloy (97% to 3% in weight) by McQueen *et al.*[16] are also shown since we do not find other static data of ultrahigh pressures.

As was mentioned in the section of calculational parameters, in our calculation, we adopt a different strategy from that by Jones *et al.*[10] in determining the energy parameters in the 0 K LAPW calculation. Although the difference in the choices of the energy parameters only results in a deviation of $\sim 1\%$ by lattice constant, it makes the calculated atomic volume be uniformly $\sim 3\%$ larger. A better way to estimate the accuracy of the calculation is to plot the curve of the reduced atomic volume V/V_0 against the pressure P. From Fig. 7(b) we can find that the comparisons between the calculations and experiments are good.

We may note again that the traditional ways for the reductions of the shock-wave data of U in Ref. 16 might be not suitable for high compressions if the thermal electronic contribution were neglected.

C. Hugoniot state

Using the calculated V_0 and E_0 of the α-U structure, the Hugoniot EOS's for U have been calculated at pressures up to 1000 GPa too, employing $\lambda=-1$, 0, and 1 for the α-U structure and $\lambda=0$ for the bct structure with $c/a=0.82$.

Shown in Fig. 8 are the calculated Hugoniot EOS's together with the measured data from the Los Alamos compilation,[12] those from the LLNL Report,[13] and the Hugoniot data (U-Mo alloy of 97% to 3% in weight) used in the reductions of shock-wave data by McQueen *et al.*[16] We especially plot the well-defined $D-u$ fitting of Ref. 12 by solid circles in Fig. 8, since the experimental data are considerably scattered in the ultrahigh pressure region. In Fig. 8(b), it is surprising that our calculated curve of P_H versus V_H/V_0 is virtually coincidental with the $D-u$ fitting of Ref. 12 at pressures up to 480 GPa.

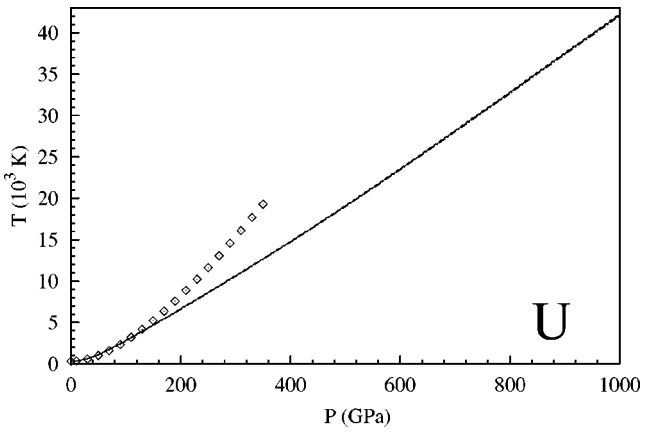

FIG. 10. The calculated temperature along the principal Hugoniot for U. The dashed, solid, and the dot-dashed lines represent the calculated results for the α-U structure using $\lambda=-1$, 0, and 1, respectively. The diamonds are the shock-reduced data (U-Mo alloy of 97% to 3% in weight) by McQueen *et al.* (Ref. 16).

D. Grüneisen gamma along the principal Hugoniot

Again, for releasing the concerns that might be raised by colleagues about the effects of the choices of the MFP in Eq. (4) on the calculated results, the calculated γ_{th}'s for α-U are depicted in Fig. 9.

E. Temperature along the principal Hugoniot

For α-U, the comparisons between the calculated Hugoniot temperatures and the shock-reduced results of Ref. 16 (U-Mo alloy of 97% to 3% in weight) are depicted in Fig. 10. We may note again that the temperatures derived by the empirical reductions are too high for ultrahigh compressions due to the neglecting of the thermal electronic contribution of F_{el} in Eq. (1).

The calculated 300 K EOS, Hugoniot EOS, and temperature along the principal Hugoniot for α-U and bct U ($c/a=0.82$) with $\lambda=0$ are listed in Table III for reference.

TABLE III. The calculated 300 K EOS, Hugoniot EOS, and Hugoniot temperature for U.

	α-U			bct [a]		
	300 K	Hugoniot		300 K	Hugoniot	
P (GPa)	V/V_0	V/V_0	T (K)	V/V_0	V/V_0	T (K)
0.0	1.0000	1.0000	300	0.9550		
20.0	0.8774	0.8804	467	0.8517		
40.0	0.8097	0.8169	842	0.7900		
60.0	0.7630	0.7752	1400	0.7438		
80.0	0.7289	0.7450	2067	0.7091		
100.0	0.7010	0.7206	2781	0.6797		
120.0	0.6784	0.7004	3524	0.6574	0.6624	1107
140.0	0.6590	0.6833	4288	0.6380	0.6503	2256
160.0	0.6416	0.6682	5058	0.6205	0.6396	3326
180.0	0.6259	0.6553	5841	0.6063	0.6296	4341
200.0	0.6121	0.6445	6636	0.5935	0.6204	5322
250.0	0.5830	0.6205	8622	0.5656	0.6000	7665
300.0	0.5595	0.6022	10 631	0.5436	0.5844	9920
350.0	0.5397	0.5879	12 683	0.5247	0.5708	12 115
400.0	0.5227	0.5755	14 764	0.5082	0.5596	14 303
450.0	0.5078	0.5644	16 882	0.4942	0.5498	16 508
500.0	0.4948	0.5542	19 050	0.4810	0.5413	18 741
600.0	0.4724	0.5382	23 515	0.4595	0.5269	23 324
700.0	0.4536	0.5257	28 119	0.4412	0.5152	28 048
800.0	0.4381	0.5151	32 795	0.4261	0.5005	32 830
900.0	0.4255	0.5056	37 490	0.4127	0.4934	37 638
1000.0	0.4140	0.4967	42 168	0.4010	0.4852	42 451

[a] $c/a=0.82$. V_0 is referred to that of α-U.

VI. SUMMARY

In summary, by means of the MFP approach in conjunction with the full-potential LAPW calculations, we have performed *ab initio* thermodynamic calculations for Th and U using their real crystal structures. The calculated properties in this paper include the 300 K static equation-of-state as well as the Hugoniot state at pressures up to 1000 GPa, which is the current frontier in high-pressure physics. We have demonstrated that the modern first-principles technique can describe most of the thermodynamic quantities within the experimental error bars even for the two heaviest $5f$ metals. In particular, by the plots of the relative volume (V/V_0) against the pressure P, the accuracy in pressure of our calculated equation-of-state might be well below 10% when compared with the experimental data available.

ACKNOWLEDGMENTS

The authors gratefully acknowledge Dr. Blaha and Professor K. Schwarz for supplying the WIEN97 code package. Valuable comments on the manuscript by Professor Zeng Zonghao are gratefully acknowledged. This work was supported by National PAN-DENG Project (Grant No. 95-YU-41).

[1] P. Hohenberg and W. Kohn, Phys. Rev. **136**, B864 (1964).
[2] W. Kohn and L.J. Sham, Phys. Rev. **140**, A1133 (1965).
[3] P. Blaha, K. Schwarz, and J. Luitz, *WIEN97, A Full Potential Linearized Augmented Plane Wave Package for Calculating Crystal Properties* (Karlheinz Schwarz, Technical Universität Wien, Austria, 1999) ISBN 3-9501031-0-4.
[4] J.P. Perdew, S. Burke, and M. Ernzerhof, Phys. Rev. Lett. **77**, 3865 (1996).
[5] M. Körling and J. Häglund, Phys. Rev. B **45**, 13 293 (1992).
[6] V. Ozolins and M. Körling, Phys. Rev. B **48**, 18 304 (1993).
[7] V.L. Moruzzi, J.F. Janak, and K. Schwarz, Phys. Rev. B **37**, 790 (1988).
[8] H.L. Skriver, O.K. Andersen, and B. Johansson, Phys. Rev. Lett. **41**, 42 (1978).

[9] P. Söderlind, Adv. Phys. **47**, 959 (1998); J.M. Wills, P.H. Andersson, L. Nordström, P. Söderlind, and O. Eriksson, cond-mat/9908344 (unpublished).
[10] M.D. Jones, J.C. Boettger, R.C. Albers, and D.J. Singh, Phys. Rev. B **61**, 4644 (2000).
[11] Y. Wang and Y. Sun, J. Phys.: Condens. Matter **12**, L311 (2000).
[12] *Los Alamos Shock Hugoniot Data*, edited by S. P. Marsh (University of California, Berkeley, 1980).
[13] *Lawrence Livemore Laboratory Report UCRL-50108*, edited by M. van Thiel (Lawrence Radiation Laboratory, University of California, Livermore, California, 1977).
[14] G. C. Kennedy and R. N. Keeler, in *American Institute of Physics Handbook*, 3rd ed., edited by D. E. Gray (McGraw Hill, New York, 1972), pp. 4–39.
[15] R.G. McQueen and S.P. Marsh, J. Appl. Phys. **31**, 1253 (1960).
[16] R. G. McQueen, S. P. Marsh, J. W. Taylor, J. N. Fritz, W. J. Carter, in *High-Velocity Impact Phenomena*, edited by R. Kinslow (Academic, New York, 1970), p. 293.
[17] Y.K. Vohra and J. Akella, Phys. Rev. Lett. **67**, 3563 (1991); Y.K. Vohra and W.B. Holzapfel, High Press. Res. **11**, 223 (1993).
[18] C.-S. Yoo, H. Cynn, and P. Söderlind, Phys. Rev. B **57**, 10 359 (1998).
[19] J. Akella, G.S. Smith, and H. Weed, J. Phys. Chem. Solids **46**, 399 (1985).
[20] J. Akella, G.S. Smith, R. Grover, Y. Wu, and S. Martin, High Press. Res. **2**, 295 (1990).
[21] Y. Wang, Phys. Rev. B **61**, R11 863 (2000).
[22] Y. Wang, D. Chen, and X. Zhang, Phys. Rev. Lett. **84**, 3220 (2000).
[23] Y. Wang and L. Li, Phys. Rev. B **62**, 196 (2000).
[24] J.S. Dugdale and D.K.C. MacDonald, Phys. Rev. **89**, 832 (1953).
[25] J. C. Slater, *Introduction to Chemical Physics* (MCGraw-Hill, New York, 1939).
[26] V.Y. Vashchenko and V.N. Zubarev, Fiz. Tverd. Tela. (Leningrad) **3**, 886 (1963) [Sov. Phys. Solid State **5**, 653 (1963)].
[27] J.A. Moriarty, Phys. Rev. B **49**, 12 431 (1994).
[28] E.R. Cowley and R.C. Shukla, Phys. Rev. B **60**, 14 500 (1999).
[29] J.C. Boettger and D.C. Wallace, Phys. Rev. B **55**, 2840 (1997).
[30] E. Wasserman, L. Stixrude, and R.E. Cohen, Phys. Rev. B **53**, 8296 (1996).
[31] C.S. Barrett, M.H. Mueller, and R.L. Hitterman, Phys. Rev. **129**, 625 (1963).
[32] J. Akella, S. Weir, J.M. Wills, and P. Söderlind, J. Phys.: Condens. Matter **9**, L549 (1997).
[33] U. Benedict, J. Less-Common Met. **128**, 7 (1987).
[34] K. A. Gschneidner, Jr., *Solid State Physics* (Academic, New York, 1964), Vol. 16, p. 275.
[35] G. Simmons and H. Wang, *Single Crystal Elastic Constants and Calculated Aggegate Properties* (MIT, Cambridge, MA, 1971), p. 307.
[36] P. Söderlind, L. Nordström, Y. Lou, and B. Johansson, Phys. Rev. B **42**, 4544 (1990).
[37] A.C. Mitchell, W.J. Nellis, J.A. Moriarty, R.A. Heinle, N.C. Homes, R.E. Tipton, and G.W. Repp, J. Appl. Phys. **69**, 2981 (1991).
[38] P. Söderlind, O. Eriksson, B. Johansson, J.M. Wills, and A.M. Boring, Nature (London) **374**, 524 (1995).